Continuum-Based Stiffened Composite Shell Element for Geometrically Nonlinear Analysis

C. L. Liao* and J. N. Reddy†
Virginia Polytechnic Institute and State University, Blacksburg, Virginia

A continuum-based, laminated, stiffened shell element is used to investigate the static, geometrically nonlinear response of composite shells. The element is developed from a three-dimensional continuum element based on the incremental, total Lagrangian formulation. The Newton-Raphson method or modified Riks method is used to trace the nonlinear equilibrium path. A number of sample problems of unstiffened and stiffened shells are presented to show the accuracy of the present element and to investigate the nonlinear response of laminated composite plates and shells.

Introduction

FINITE-ELEMENT analyses of the large displacement theories are based on the principle of virtual work or the associated principle of stationary potential energy. Horrigmoe and Bergan[1] presented classical variational principles for nonlinear problems by considering incremental deformations of a continuum. A survey of various principles in incremental form in different reference configurations, such as the total Lagrangian and updated Lagrangian formulations, is presented by Wünderlich.[2] In the total Lagrangian description, all static and kinematic variables are referred to the initial configuration. Finite-element models based on such formulations have been used in the analysis of arch and shell instability problems.[3-6] A special numerical technique must be adopted to trace the path of the load-deflection curve near the limit point (i.e., critical buckling load) and in the postbuckling region, because the stiffness matrix in the vicinity of the limit point is nearly singular, and the descending branch of the load-deflection curve in the postbuckling region is characterized by a negative-definite stiffness matrix. Many methods have been proposed to solve limit-point problems. Among these are the simple methods of suppressing equilibrium iterations,[7,8] the introduction of artificial spring,[3] the displacement control method,[7,8] and the "constant-arc-length method" of Riks.[11,12] Reviews of these most commonly used techniques are contained in Refs. 13 and 14. Among these methods, the modified Riks method appears to be the most effective in conjunction with the finite-element method. Many investigators[11-15] have used this method in its original or modified form to determine the pre- and postbuckling behavior of various types of structures such as arches, shells, and domes. In most of these works, only isotropic material was considered. Very few works of the nonlinear buckling analysis of laminated composite structures are reported in the literature.[16]

When solving the problems of shells with stiffeners by the finite-element method, a beam element whose displacement pattern is compatible with that of the shell is required. In analyzing eccentrically stiffened cylindrical shell, Kohnke and Schnobrich[17] proposed a 16-deg-of-freedom (DOF) isotropic beam finite element that has displacements compatible with the cylindrical shell element from which the beam element is reduced. Venkatesh and Rao[18] have presented a laminated anisotropic stiffener element, which is used to solve problems of laminated anisotropic shells stiffened by laminated anisotropic stiffeners.

In Refs. 17 and 18, the shell and beam elements are all based on the classical thin shell and beam theories. Therefore, the transverse shear deformation is neglected. Bathe and Bolourchi[19] employed Ahmad thick shell elements in conjunction with the degenerated three-dimensional beam elements to model an isotropic stiffened plate in which the transverse shear deformations are included. But in all of these works only linear static analysis is considered. Postbuckling analysis of composite laminates using two-dimensional plate theories can be found in Refs. 20–22. A review of the literature reveals that there is a need for comparison and assessment of transverse shear deformation plate theory and classical plate theory as well as comparisons with discrete stiffener approach. The present study was undertaken to develop a laminated, stiffened composite shell element for geometric nonlinear analysis using a continuum-based stiffened shell element. Both the basic shell element and the curved beam element used to model stiffeners are derived from the three-dimensional continuum element.

Formulation

Consider the motion of a body in a fixed Cartesian coordinate system and assume that the body can experience large displacements and rotations. Suppose that solutions for kinematic and static variables for all load steps prior to the current one have been obtained, and that the solution for the next load step is sought (see Fig. 1).

Because the displacement-based finite-element procedure will be employed for numerical solution, the principle of virtual displacements is used to express the equilibrium of the body in the configuration C_2. In the present study, left subscripts and superscripts on a quantity are used to indicate, respectively, the configuration to which the quantity is referred, and the configuration in which the quantity is measured. The principle of virtual displacements requires that

$$\int_{{}^2V} {}^2\tau_{ij}\, \delta_2 e_{ij}\, \mathrm{d}V = {}^2R \tag{1}$$

where

${}^2\tau_{ij}$ = Cartesian components of the Cauchy stress tensor in C_2 (the Cauchy stresses are always referred to the configuration in which they occur: ${}^2\tau_{ij} \equiv {}^2_2\tau_{ij}$)

Received Aug. 20, 1987; revision received May 27, 1988.

*Graduate Research Assistant; currently Assistant Professor, Department of Mechanical Engineering, National Taiwan Institute of Technology, Taiwan.

†Clifton C. Garvin Professor, Department of Engineering Science and Mechanics.

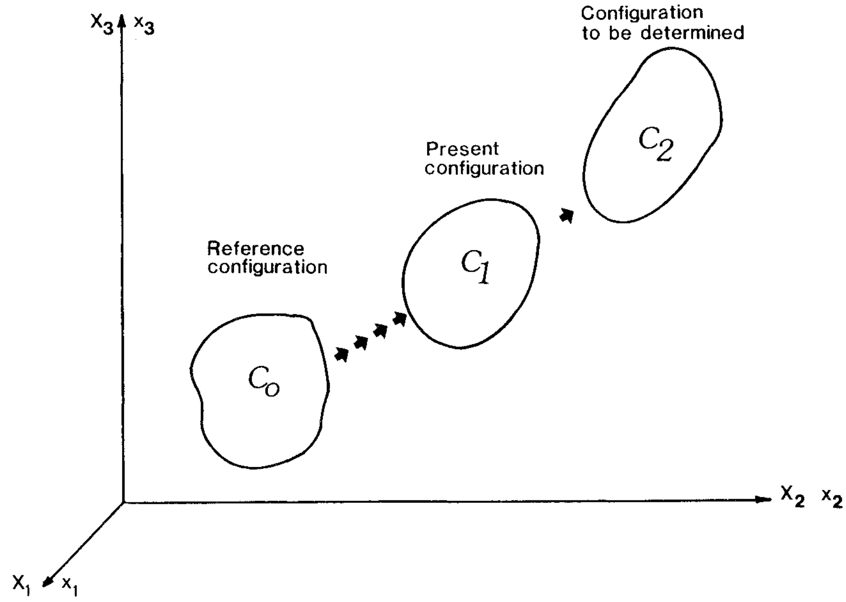

Fig. 1 Total Lagrangian description of a continuous medium.

${}_2e_{ij}$ = Cartesian components of the infinitesimal strain tensor associated with the displacements u_i in going from the configuration c_1 to the configuration c_2, i.e., ${}_2e_{ij} = \frac{1}{2}[(\partial u_i/\partial x_j) + (\partial u_j/\partial x_i)]$, which are also referred to configuration c_2

x_i = Cartesian components of a point in configuration c_2

${}^2R$ = work done by external loads

$$ {}^2R = \int_{{}^2A} {}^2_2t_k \, \delta u_k \, \mathrm{d}A + \int_{{}^2V} {}^2\rho {}^2_2f_k \, \delta u_k \, \mathrm{d}V \tag{2} $$

Here ${}^2_2t_k$ and ${}^2_2f_k$ denote the components of externally applied surface and body-force vectors, respectively, δu_k denotes virtual variation in the current displacement components ${}^2u_k$, and δ_2e_{ij} denotes virtual variations in strains. The area and volume elements $\mathrm{d}A$ and $\mathrm{d}V$ are assumed to be in the configuration indicated on the integral.

An approximate solution of Eq. (1) can be obtained by referring all variables to a previously calculated known equilibrium configuration and linearizing the resulting equation. This solution is then improved by iteration. The applied forces in Eq. (2) are evaluated using

$$ {}^2_2t_k \, {}^2(\mathrm{d}A) = {}^2_0t_k \, {}^0(\mathrm{d}A) $$

$$ {}^2\rho \, {}^2_2f_k \, {}^2(\mathrm{d}V) = {}^0\rho \, {}^2_0f^0_k \, {}^0(\mathrm{d}V) \tag{3} $$

The volume integral of the product of the Cauchy stress and the variation of infinitesimal strain in Eq. (1) can be transformed to give

$$ \int_{{}^2V} {}^2\tau_{ij} \, \delta_2e_{ij} \, \mathrm{d}V = \int_{{}^0V} {}^2_0S_{ij} \, \delta^2_0\epsilon_{ij} \, \mathrm{d}V \tag{4} $$

where

${}^2_0S_{ij}$ = Cartesian components of the second Piola-Kirchhoff stress tensor corresponding to configuration c_2, but measured in the configuration c_0

${}^2_0\epsilon_{ij}$ = Cartesian components of the Green-Lagrange strain tensor in the configuration c_2 referred to the configuration c_0, and ${}^2_0\epsilon_{ij}$ are defined as ${}^2_0\epsilon_{i,j} = (1/2)({}^2_0u_{i,j} + {}^2_0u_{i,j} + {}^2_0u_{k,i} \, {}^2_0u_{k,j})$, ${}^2_0u_{i,j} = (\partial^2u_i/\partial X_j)$

${}^2u_i$ = components of displacement vector from initial configuration c_0 to configuration c_2: ${}^2u_i = {}^2x_i - X_i$

Because the stresses ${}^2_0S_{ij}$ and strains ${}^2_0\epsilon_{ij}$ are unknown, the following incremental decompositions are used:

$$ {}^2_0S_{ij} = {}^1_0S_{ij} + {}_0S_{ij} \tag{5} $$

$$ {}^2_0\epsilon_{ij} = {}^1_0\epsilon_{ij} + {}_0\epsilon_{ij} \tag{6} $$

where ${}^1_0S_{ij}$ and ${}^1_0\epsilon_{ij}$ are the known second Piola-Kirchhoff stresses and Green-Lagrange strains in the configuration c_1. Using the definition of the Green-Lagrange strain tensor and ${}^2u_i = {}^1u_i + u_i$, where u_i = the increment in displacement components, it follows that

$$ {}_0\epsilon_{ij} = {}_0e_{ij} + {}_0\eta_{ij} \tag{7} $$

where

$$ {}_0e_{ij} = \tfrac{1}{2}({}_0u_{i,j} + {}_0u_{j,i} + {}^1_0u_{k,i} \, {}_0u_{k,j} + {}_0u_{k,i} \, {}^1_0u_{k,j}) \tag{8} $$

= linear part of strain increment ${}_0\epsilon_{ij}$,

$$ {}_0\eta_{ij} = \tfrac{1}{2} \, {}_0u_{k,i} \, {}_0u_{k,j} \tag{9} $$

= nonlinear part of strain increment ${}_0\epsilon_{ij}$, and $\delta^2_0\epsilon_{ij} = \delta^1_0\epsilon_{ij} + \delta_0\epsilon_{ij} = \delta_0\epsilon_{ij}$, since ${}^1_0\epsilon_{ij}$ are already known. The incremental second Piola-Kirchhoff stress components ${}_0S_{ij}$ are related to the incremental Green-Lagrange strain components ${}_0\epsilon_{ij}$ through the constitutive tensor components ${}_0C_{ijrs}$,

$$ {}_0S_{ij} = {}_0C_{ijrs} \, {}_0\epsilon_{rs} \tag{10} $$

Using Eqs. (3–10), Eq. (1) can be written as

$$ \int_{{}^0V} {}_0C_{ijrs} \, {}_0\epsilon_{rs} \, \delta_0\epsilon_{ij} \, {}^0\mathrm{d}V + \int_{{}^0V} {}^1_0S_{ij} \, \delta_0\eta_{ij} \, {}^0\mathrm{d}V $$

$$ = {}^2R - \int_{{}^0V} {}^1_0S_{ij} \, \delta_0e_{ij} \, {}^0\mathrm{d}V \tag{11} $$

which represents a nonlinear equilibrium equation for the incremental displacements u_i.

The solution of Eq. (11) cannot be calculated directly since they are nonlinear in the displacement increments. Approximate solution can be obtained by assuming that ${}_0\epsilon_{ij} = {}_0e_{ij}$ in Eq. (11). This means that in addition to using $\delta_0\epsilon_{ij} = \delta_0 e_{ij}$, the incremental constitutive relation

$$ {}_0S_{ij} = {}_0C_{ijrs}\,{}_0e_{rs} $$

is used. Hence, in the total Lagrangian formulation, the approximate equation to be solved is

$$ \int_{{}^0V} {}_0C_{ijrs}\,{}_0e_{rs}\,\delta_0 e_{ij}\,{}^0\mathrm{d}V + \int_{{}^0V} {}_0^1S_{ij}\,\delta_0\eta_{ij}\,{}^0\mathrm{d}V = {}^2R - \int_{{}^0V} {}_0^1S_{ij}\,\delta_0 e_{ij}\,{}^0\mathrm{d}V \tag{12} $$

Finite-Element Model

The coordinates and displacements are interpolated using the same interpolation functions (i.e., isoparametric formulation is used), so that the displacement compatibility across element boundaries is preserved in all configurations. Hence,

$$ X = \sum_{k=1}^{n} \Psi_k X_i^k, \qquad x_i = \sum_{k=1}^{n} \Psi_k x_i^k, \qquad i = 1,2,3 $$

$$ {}^1u_i = \sum_{k=1}^{n} \Psi_k\,{}^1u_i^k, \qquad u_i = \sum_{k=1}^{n} \Psi_k u_i^k, \qquad i = 1,2,3 \tag{13} $$

where Ψ_k is the interpolation function corresponding to nodal point k, and n is the number of element nodal points.

Using Eqs. (13) to evaluate the displacement derivatives required in the integrals, Eq. (12) can be expressed as

$$ [{}_0^1(K_L) + {}_0^1(K_{NL})]\ \{\Delta^e\} = {}^2\{R\} - {}_0^1\{F\} \tag{14} $$

where $\{\Delta^e\}$ is the vector of nodal incremental displacements from c_1 to c_2 in an element, and (see Bathe[23])

$$ {}_0^1[K_L] = \int_{{}^0V} {}_0^1[B_L]^T\,{}_0[C]\,{}_0^1[B_L]\,{}^0\mathrm{d}V \tag{15a} $$

$$ {}_0^1[K_{NL}] = \int_{{}^0V} {}_0^1[B_{NL}]^T\,{}_0^1[S]\,{}_0^1[B_{NL}]\,{}^0\mathrm{d}V \tag{15b} $$

$$ {}_0^1\{F\} = \int_{{}^0V} {}_0^1[B_L]^T\,{}_0^1\{\hat{S}\}\,{}^0\mathrm{d}V \tag{15c} $$

In the above equations, ${}_0^1[B_L]$ and ${}_1^0[B_{NL}]$ are linear and nonlinear strain-displacement transformation matrices, ${}_0[C]$ is the incremental stress-strain material property matrix, ${}_0^1[S]$ is a matrix of second Piola-Kirchhoff stress components, and ${}_0^1\{\hat{S}\}$ is a vector of these stresses. All matrix elements correspond to the configuration c_1 are defined with respect to the configuration c_0.

It is important to note that Eq. (14) yields only an approximation to the actual solution to be obtained in each load step. Therefore, it may be necessary to iterate in each step until Eq. (1) is satisfied to a required tolerance. In the present study, either the Newton-Raphson or the Riks iterative technique is used to determine the equilibrium solution.

The shell element and the stiffener beam elements are obtained by imposing appropriate kinematic constraints on the three-dimensional isoparametric solid element. The beam element exhibits the displacement compatibility with the shell element and has the transverse shear deformation and variable thickness properties. Also, with the introduction of offsets of the beam neutral axis from the reference axis in the element formulation, three-dimensional stiffeners and curved beams of general cross section may be modeled.[24] For detailed derivation of these individual elements, the reader is referred to Refs. 23 and 24. The main contribution of the present study is to account for laminate constitutive relations in the development of the shell and its stiffeners.

The material stiffness matrix ${}_0[C']$ [see Eqs. (15)] for the kth lamina of a laminated composite shell in the local coordinate system (x_1', x_2', x_3') can be expressed as[25]

$$ {}_0[C']_{(k)} = \begin{bmatrix} C_{11}' & C_{12}' & C_{16}' & 0 & 0 \\ C_{12}' & C_{22}' & C_{26}' & 0 & 0 \\ C_{16}' & C_{26}' & C_{36}' & 0 & 0 \\ 0 & 0 & 0 & C_{44}' & C_{45}' \\ 0 & 0 & 0 & C_{45}' & C_{55}' \end{bmatrix} \tag{16} $$

where

$$ C_{11}' = m^4Q_{11} + 2m^2n^2(Q_{12} + 2Q_{66}) + n^4Q_{22} $$

$$ C_{12}' = m^2n^2(Q_{11} + Q_{22} - 4Q_{66}) + (m^4 + n^4)Q_{12} $$

$$ C_{16}' = mn[m^2Q_{11} - n^2Q_{22} - (m^2 - n^2)(Q_{12} + 2Q_{66})] $$

$$ C_{22}' = n^4Q_{11} + 2m^2n^2(Q_{12} + 2Q_{66}) + m^4Q_{22} $$

$$ C_{26}' = mn[n^2Q_{11} - m^2Q_{22} + (m^2 - n^2)(Q_{12} + 2Q_{66})] $$

$$ C_{66}' = m^2n^2(Q_{11} + Q_{22} - 2Q_{12}) + (m^2 - n^2)^2Q_{66} $$

$$ C_{55}' = m^2Q_{55} + n^2Q_{44}, \quad C_{45}' = mn(Q_{55} - Q_{44}) $$

$$ C_{44}' = m^2Q_{44} + n^2Q_{55} $$

$$ m = \cos\theta_{(k)}, \qquad n = \sin\theta_{(k)} \tag{17} $$

and Q_{ij}, which are the plane stress-reduced stiffnesses of an orthotropic lamina in the material coordinate system, are reduced from the constitutive relations for three-dimensional orthotropic body by neglecting the normal stress in the thickness direction. The Q_{ij} can be expressed in terms of engineering constants of a lamina as

$$ Q_{11} = \frac{E_1}{1 - \nu_{12}\nu_{21}}, \quad Q_{12} = \frac{\nu_{12}E_2}{1 - \nu_{12}\nu_{21}}, \quad Q_{22} = \frac{E_2}{1 - \nu_{12}\nu_{21}} $$

$$ Q_{55} = (G_{13})K, \quad Q_{44} = (G_{23})K, \quad Q_{66} = G_{12} \tag{18} $$

where K is the shear correction coefficient, which is taken to be equal to 5/6, and it is assumed that $E_3 = E_2$ and $\nu_{12} = \nu_{13}$.

To evaluate element matrices in Eqs. (15), we employ the Gaussian quadrature. Because we are dealing with laminated composite structures, the constitutive matrix ${}_0[C]$ is different from layer to layer and is not a continuous function in the thickness direction; hence, the integration should be performed separately for each layer. The Jacobian matrix, in general, is a function of ξ, η, and ζ. The terms in ζ may be neglected provided the thickness-to-curvature ratios are small. Then the Jacobian matrix ${}^0[J]$ becomes independent of ζ, and explicit integration can be employed. If ζ terms are retained in ${}^0[J]$, Gaussian points through the thickness should be added. In the present study, we assume that the Jacobian matrix is independent of ζ in the evaluation of element matrices and the internal nodal force vector. For thin shell structures, in order to avoid "element shear locking" we use reduced integration scheme to evaluate the stiffness coefficients associated with the transverse shear strains.

If a shell element is subjected to a distributed load (such as the weight or pressure), the corresponding load vector ${}^2\{R\}$ is given by

$$^2\{R\} = \int_{^0A} {}^1[H]^T \begin{Bmatrix} ^2P_1 \\ ^2P_2 \\ ^2P_3 \end{Bmatrix} \mathrm{d}A \tag{19}$$

where

^2P_i = the component of distributed load in the X_i direction in configuration c_2

^0A = the area of upper or middle or bottom surface of the shell element, depending on the position of the loading.

The loading is assumed to be deformation-independent.

Numerical Results

A number of representative problems were analyzed using the composite shell element developed in the present study. Some of the problems have been analyzed in the literature using different finite-element models. Comparisons of present results with available solutions show the accuracy of the element. Additional problems of composite plates and shells are presented to show the effects of shear deformation, geometric stiffening, and nonlinearity, and lamination scheme on deflections.

Clamped Shallow Circular Arch Subjected to a Center-Point Load

The geometry of this arch is shown in Fig. 2. The material properties and geometric parameters used are

$$E = 6.895 \times 10^4 \text{ N/mm}^2$$
$$\nu = 0.25$$
$$R = 2540 \text{ mm}$$
$$h = 50.8 \text{ mm}$$
$$\text{width} = 25.4 \text{ mm}$$
$$\theta = 0.245 \text{ rad}$$
$$\text{load parameter } \bar{P} = (PR^2\theta/\pi^2 EI)10 \tag{20}$$

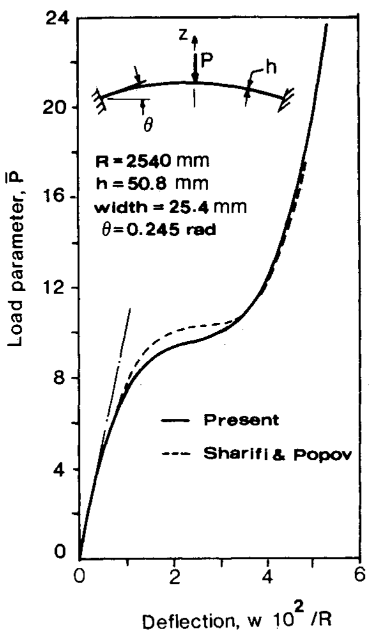

Fig. 2 Large deflection behavior of a clamped arch under a central-point load.

Because of the symmetry of geometry and loading, only one-half of the arch is modeled with four three-node beam elements. The results of the present study are compared in Fig. 2 with the results of Sharifi and Popov,[3] who used 10 two-node planar beam elements and the updated Lagrangian formulation. The small difference between the solutions is attributed to the difference in the formulations used.

Symmetrical Buckling of Isotropic Shallow Arches

Two shallow-arch examples, investigated by Sharifi and Popov,[3] are analyzed using the present nonlinear finite-element model. The modified Riks method is used as the solution procedure to obtain the nonlinear responses. The geometries and loadings of both arches are shown in Figs. 3 and 4, respectively. The material properties and geometric parame-

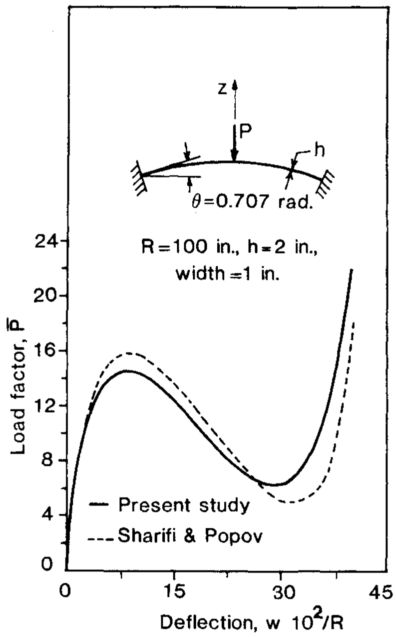

Fig. 3 Symmetrical buckling of a shallow, clamped arch under a central-point load.

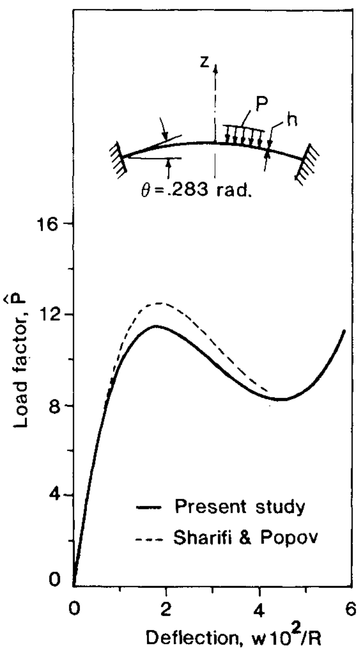

Fig. 4 Symmetrical buckling of a shallow, clamped arch under uniformly distributed load.

ters used are

$$E = 10^7 \text{ psi}, \ \nu = 0.25$$

$$R = 100 \text{ in.}, \ h = 2 \text{ in.}, \ \text{width} = 1 \text{ in.}, \ \theta = 0.707 \text{ rad} \tag{21}$$

Arch 1 is subjected to a center-point load, while arch 2 is under a uniform loading. In each case, due to the symmetry, only one-half of the arch was modeled with five three-node beam elements. The present results are compared with those in Ref. 3 in Figs. 3 and 4. The load parameters used for arch 2 is $\hat{P} = \bar{P}R\theta$, with $\theta = 0.283$ rad. To obtain the postbuckling response, Sharifi and Popov[3] used the method of fictitious elastic springs. The difference between the two solutions is largely due to the discrete stiffness used in Ref. 3.

Symmetrical Buckling of Laminated Shallow Arches

The geometries and loading of these two two-layer composite arches are the same as that of arch 1 in the last problem. The material properties used are

$$E_1/E_2 = 25, \ E_2 = 10^6 \text{ psi}, \ G_{12}/E_2 = 0.5, \ G_{13} = G_{12}$$

$$G_{23}/E_2 = 0.2, \ \nu_{12} = 0.25 \tag{22}$$

Since the symmetrical deformation modes exist for both cross-ply (0/90) and angle-ply (−45/45) arches, only one-half of the arch was molded using three-node beam elements for each beam. The nonlinear responses obtained in the present study with the modified Riks method are shown in Fig. 5. Note that the two-layer cross-ply arch is much stiffer than the two-layer angle-ply arch.

Simply-Supported Spherical Shell Subjected to a Point Load

The isotropic shell shown in Fig. 6 was analyzed for its large displacement response with 4 nine-node elements and 16 four-node elements modeling one-quarter of the shell. The following geometric and material parameters are used:

$$R = 100 \text{ in.}, \ a = 30.9017 \text{ in.}, \ h = 3.9154 \text{ in.}$$

$$E = 10^4 \text{ psi}, \ \nu = 0.3 \tag{23}$$

The boundary conditions used are

$$u = \phi_1 = 0 \text{ on } x_1 = 0, \qquad u = v = w = \phi_2 = 0 \text{ on } x_1 = a$$

$$v = \phi_2 = 0 \text{ on } x_2 = 0, \qquad u = v = w = \phi_1 = 0 \text{ on } x_2 = a \tag{24}$$

Figure 6 contains plots of the load-deflection curves obtained using the shell element. The modified Riks method automatically determines the load increments. Figure 6 also includes the results of Bathe and Ho.[26] Note that the element developed by Bathe and Ho[26] is stiffer than the continuum element.

Shallow Cylindrical Shell with a Center Point

The isotropic shallow cylindrical shell (hinged at the longitudinal edges and free at the curved boundaries) shown in Fig. 7 is analyzed. One-quarter of the shell was analyzed with 4 nine-node degenerated shell elements. The geometric and material parameters used are

$$R = 2540 \text{ mm}, \ a = 254 \text{ mm}, \ h = 6.35 \text{ mm}$$

$$E = 3.103 \text{ kN/mm}^2, \ \nu = 0.3 \tag{25}$$

The symmetry and hinged boundary conditions used are the same as those in Eq. (24). The structure exhibits snap-through and snap-back phenomena. The solution obtained by Crisfield[14] is also shown in Fig. 7. The present results are in excellent agreement.

Simply-Supported Spherical Shell with Symmetrical Stiffeners

The geometry of the stiffened spherical shell is shown in Fig. 8. The material properties and geometric parameters used are the same as those in Eqs. (23). Because of the symmetry, only one-quarter of the stiffened shell was modeled with 16

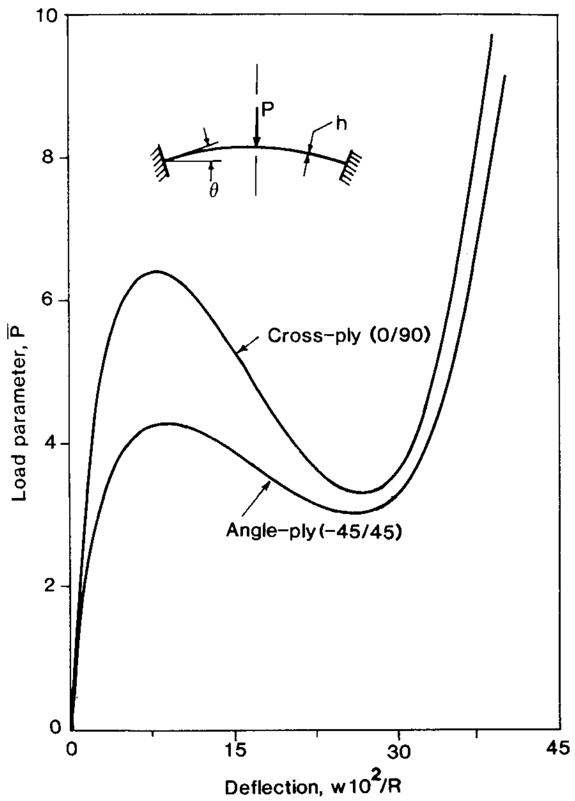

Fig. 5 Geometrically nonlinear response of laminated, clamped arches under central-point load (see Fig. 3 for geometry).

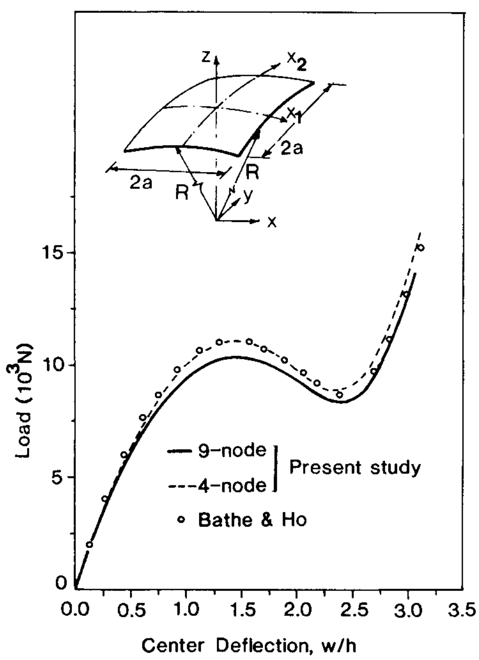

Fig. 6 Geometrically nonlinear response of an isotropic, simply supported spherical panel under central-point load.

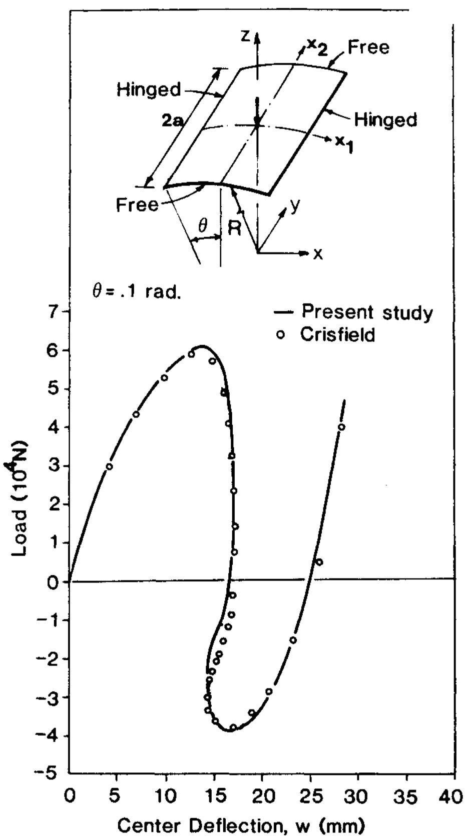

Fig. 7 Geometrically nonlinear response of an isotropic, shallow cylindrical shell panel under center-point load.

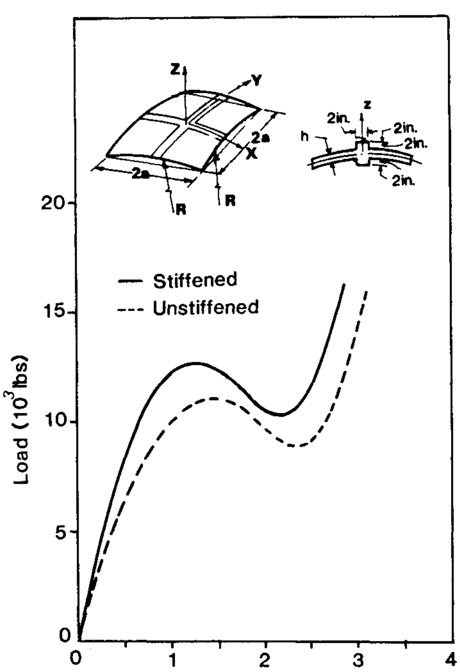

Fig. 8 Geometrically nonlinear response of isotropic, spherical panels with and without stiffeners and subjected to central-point load.

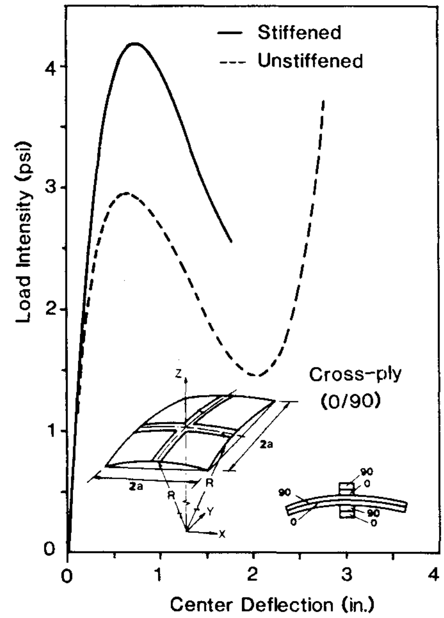

Fig. 9 Geometrically nonlinear responses of a cross-ply (0/90) laminated spherical and with and without laminated stiffeners and subjected to external pressure.

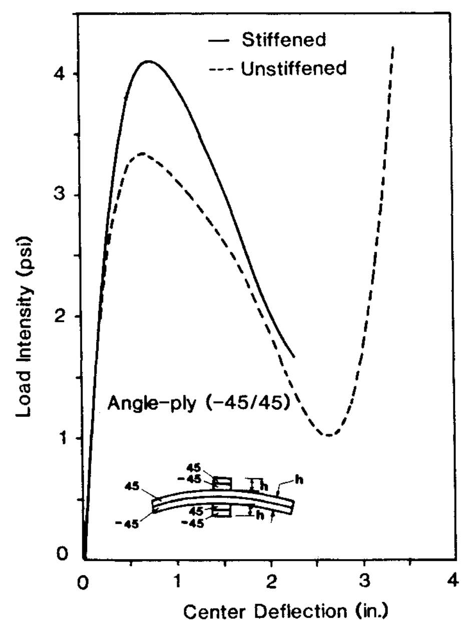

Fig. 10 Geometrically nonlinear response of an angle-ply (− 45/45) laminated spherical panel with and without laminated stiffeners and subjected to external pressure.

four-node shell elements and 16 two-node beam elements. In addition to the boundary conditions in Eqs. (24), $\phi_3 = 0$ is used on all edges. The geometric nonlinear responses of the stiffened shell and the same shell without stiffeners (and subjected to a center-point load) are shown in Fig. 8. The same nonstiffened shell was analyzed by Bathe and Ho,[27] who used a flat three-node triangular shell element which includes transverse shear deformation. The present results are found to be in good agreement with those of Bathe and Ho. The stiffened shell buckles under a center-point load. The effect of stiffeners is to increase the limit load, but the form of the load-deflection curve remains essentially the same.

Two-Layer Cross-Ply and Angle-Ply Stiffened Shell Panels

The geometries of the two stiffened laminated spherical shells and the stacking sequences are shown in Figs. 9 and 10. The material properties and geometric parameters used are

$$E_1/E_2 = 25,\ E_2 = 10^6 \text{ psi},\ \nu_{12} = 0.25,\ G_{12}/E_2 = 0.5$$

$$G_{13} = G_{12},\ G_{23}/E_2 = 0.2$$

$$R = 1000 \text{ in.},\ h = 1 \text{ in.},\ a = 50 \text{ in.}$$

The shell panels are simply-supported and are subjected to uniform internal pressure. The boundary conditions used are the same as those in the last problem for the cross-ply shell, and u and v are interchanged in the boundary conditions (24) for the angle-ply shell. One-quarter of each stiffened shell was modeled with 4 nine-node shell elements and 8 three-node beam elements. The geometric nonlinear responses of these two shells with and without stiffeners are shown in Figs. 9 and 10, respectively. The effect of stiffeners is to increase the limit-load values. The load-deflection curves for stiffened shells are terminated beyond the limit load to save computational time.

Summary and Conclusions

A continuum shell element with compatible stiffeners is developed for the geometric nonlinear analysis of laminated, stiffened shell structures. The elements are essentially the same as in Ref. 23, except for the inclusion of laminated anisotropic material behavior. A number of sample problems are analyzed to both validate the present element and bring out the effects of lamination scheme, geometric nonlinearity, and stiffeners. The numerical examples demonstrate the validity and efficiency of the present element. A composite transition element to model transition regions between a three-dimensional continuum element and the two-dimensional continuum shell element was developed recently by the authors,[28] completing a library of continuum elements for global-local analysis of practical problems.

References

[1]Horrigmoe, G. and Bergan, P. G., "Incremental Variational Principle and Finite Element Models for Nonlinear Problems," *Computer Methods in Applied Mechanics and Engineering,* Vol. 7, 1976, pp. 201–217.

[2]Wünderlich, W., "Incremental Formulations for Geometrically Nonlinear Problems," *Formulations and Algorithm in Finite Element Analysis,* edited by K. J. Bathe, J. T. Oden, and W. Wünderlich, M.I.T. Press, Cambridge, MA, 1977, pp. 193–239.

[3]Sharifi, P. and Popov, E. P., "Nonlinear Buckling Analysis of Sandwich Arches," *Journal of Engineering Mechanics Division, ASCE,* Vol. 97, 1981, pp. 1397–1411.

[4]Walker, A. C., "A Nonlinear Finite Element Analysis of Shallow Circular Arches," *International Journal of Solids and Structures,* Vol. 5, 1969, pp. 97–107.

[5]Noor, A. K., Greene, W. H., and Hartley, S. J., "Nonlinear Finite Element Analysis of Curved Beams," *Computer Methods in Applied Mechanics and Engineering,* Vol. 12, 1977, pp. 289–307.

[6]Noor, A. K. and Peters, J. M., "Mixed Models and Reduced/Selective Integration Displacement Models for Nonlinear Analysis of Curved Beams," *International Journal for Numerical Methods in Engineering,* Vol. 17, 1981, pp. 615–631.

[7]Bergan, P. G., Horrigmoe, G., Krakeland, B., and Soreide, T. H., "Solution Techniques for Nonlinear Finite Element Problems," *International Journal for Numerical Methods in Engineering,* Vol. 12, 1978, pp. 1677–1696.

[8]Bergan, P. G. and Soreide, T. H., "Solution of Large Displacement and Instability Problems Using the Current Stiffness Parameter," *Finite Elements in Nonlinear Mechanics,* Tapir Press, 1978, pp. 647–649.

[9]Argyris, J. H., "Continua and Discontinua," *Proceedings of the 1st Conference on Matrix Methods in Structural Mechanics,* Wright-Patterson Air Force Base, OH, 1965, pp. 11–189.

[10]Batoz, J. L. and Dhatt, G., "Incremental Displacement Algorithms for Nonlinear Problems," *International Journal for Numerical Methods in Engineering,* Vol. 14, 1979, pp. 1262–1266.

[11]Rics, E., "On the Numerical Solution of Snapping Problems in the Theory of Elastic Stability," Stanford Univ., Stanford, CA, Rept. SUDDAR No. 401, Aug. 1970.

[12]Riks, E., "An Incremental Approach to the Solution of Snapping and Buckling Problem," *International Journal of Solids and Structures,* Vol. 15, 1979, pp. 529–551.

[13]Ramm, E., "Strategies for Tracing the Nonlinear Response Near Limit Points," *Nonlinear Finite Element Analysis in Structural Mechanics,* edited by W. Wünderlich, M. Stein, K. J. Bathe, Springer-Verlag, Berlin, 1981, pp. 63–89.

[14]Crisfield, M. A., "A Fast Incremental/Iterative Solution Procedure That Handles Snap-Through," *Computers and Structures,* Vol. 13, 1981, pp. 55–62.

[15]Bathe, K. J. and Dvorkin, E. N., "On the Automatic Solution of Nonlinear Finite Element Equations," *Computers and Structures,* Vol. 17, 1983, pp. 871–879.

[16]Stanley, G. M. and Felippa, C. A., "Computational Procedures for Postbuckling of Composite Shells," *Finite Element Methods for Nonlinear Problems,* edited by P. G. Bergan, K. J. Bathe, and W. Wünderlich, Springer-Verlag, Berlin, 1986, pp. 357–385.

[17]Kohnke, P. C. and Schnobrich, W. C., "Analysis of Eccentrically Stiffened Cylindrical Shells," *ASCE Journal of the Structural Division,* Vol. 98, 1972, pp. 1393–1510.

[18]Venkatesh, A. and Rao, K. P., "Analysis of Laminated Shells of Revolution with Laminated Stiffeners Using a Doubly Curved Quadrilateral Finite Element," *Computers and Structures,* Vol. 20, 1985, pp. 669–682.

[19]Bathe, K. J. and Bolourchi, S., "A Geometric and Material Nonlinear Plate and Shell/ Element," *Computers and Structures,* Vol. 11, 1980, pp. 23–48.

[20]Snell, M. G. and Morley, N. T., "The Compression Buckling Behavior of Highly Curved Panels of Carbon Fibre Reinforced Plastic," *Proceedings of the 5th International Conference on Composite Materials,* ICCM, Vol. 5, Aug. 1985, pp. 1327–1354.

[21]Rohwer, K., "Nachbeulverhalten von Platten und Schalenfeldern aus Faserverbundstoff," *Zeitschrift fuer Flugwissenschaften und Weltraumforschung,* Vol. 10, July–Aug. 1986, pp. 228–235.

[22]Knight, N. F., Jr., and Starnes, J. H., Jr., "Postbuckling Behavior of Axially Compressed Graphite-Epoxy Cylindrical Panels with Circular Holes," *Journal of Pressure Vessel Technology,* Vol. 107, Nov. 1985, pp. 394–402.

[23]Bathe, K. J., *Finite Element Procedures in Engineering Analysis,* Prentice-Hall, Englewood Cliffs, NJ, 1982.

[24]Ferguson, G. H. and Clark, R. H., "A Variable Thickness Curved Beam and Shell Stiffening Element with Shear Deformations," *International Journal for Numerical Methods in Engineering,* Vol. 14, 1979, pp. 581–592.

[25]Reddy, J. N., *Energy and Variational Methods in Applied Mechanics,* Wiley, New York, 1984.

[26]Bathe, K. J. and Ho, L. W., "A Simple Effective Element for Analysis of General Shell Structures," *Computers and Structures,* Vol. 13, 1981, pp. 673–681.

[27]Bathe, K. J. and Ho, L. W., "Some Results in the Analysis of Thin Shell Structures," *Nonlinear Finite Element Analysis in Structural Mechanics,* edited by W. Wünderlich, M. Stein, K. J. Bathe, Springer-Verlag, Berlin, 1981, pp. 122–150.

[28]Liao, C. L., Reddy, J. N., and Engelstand, S. P., "A Solid-Shell Transition Element for Geometrically Nonlinear Analysis of Laminated Composite Structures," *International Journal for Numerical Methods in Engineering,* Vol. 26, 1988, pp. 1843–1854.